

Published in final edited form as:

Nat Neurosci. 2011 March ; 14(3): 387–397. doi:10.1038/nn.2749.

## An optogenetic toolbox designed for primates

Ilka Diester<sup>1</sup>, Matthew T Kaufman<sup>2</sup>, Murtaza Mogri<sup>1</sup>, Ramin Pashaie<sup>1,6</sup>, Werapong Goo<sup>1</sup>, Ofer Yizhar<sup>1</sup>, Charu Ramakrishnan<sup>1</sup>, Karl Deisseroth<sup>1,2,3,4</sup>, and Krishna V Shenoy<sup>1,2,5</sup>

<sup>1</sup>Department of Bioengineering, Stanford University, Stanford, California, USA

<sup>2</sup>Neurosciences Program, Stanford University, Stanford, California, USA

<sup>3</sup>Department of Psychiatry and Behavioral Sciences, Stanford University, Stanford, California, USA

<sup>4</sup>Howard Hughes Medical Institute, Stanford University, Stanford, California, USA

<sup>5</sup>Department of Electrical Engineering, Stanford University, Stanford, California, USA

### Abstract

Optogenetics is a technique for controlling subpopulations of neurons in the intact brain using light. This technique has the potential to enhance basic systems neuroscience research and to inform the mechanisms and treatment of brain injury and disease. Before launching large-scale primate studies, the method needs to be further characterized and adapted for use in the primate brain. We assessed the safety and efficiency of two viral vector systems (lentivirus and adeno-associated virus), two human promoters (human synapsin (*hSyn*) and human thymocyte-1 (*hThy-1*)) and three excitatory and inhibitory mammalian codon-optimized opsins (channelrhodopsin-2, enhanced *Natronomonas pharaonis* halorhodopsin and the step-function opsin), which we characterized electrophysiologically, histologically and behaviorally in rhesus monkeys (*Macaca mulatta*). We also introduced a new device for measuring *in vivo* fluorescence over time, allowing minimally invasive assessment of construct expression in the intact brain. We present a set of optogenetic tools designed for optogenetic experiments in the non-human primate brain.

---

Systems neuroscience relies mainly on recordings of neural activity and its correlation with behavior. It also uses pharmacological manipulations to perturb the neural system and thereby to establish causal relationships between neural activity and behavior. These manipulations can be targeted to specific cell types and are very powerful<sup>1</sup>, but they act on a time scale of minutes, whereas neurons act on a time scale of milliseconds. Electrical

---

© 2011 Nature America, Inc. All rights reserved.

Correspondence should be addressed to K.D. (deissero@stanford.edu) or K.V.S. (shenoy@stanford.edu).

<sup>6</sup>Present address: Department of Electrical Engineering and Computer Science, University of Wisconsin-Milwaukee, Milwaukee, Wisconsin, USA.

Note: Supplementary information is available on the Nature Neuroscience website.

### AUTHOR CONTRIBUTIONS

I.D., K.V.S. and K.D. conceived and designed the experiments. I.D. wrote the manuscript and all authors contributed to its editing. I.D. conducted all experiments, histological analysis and data analysis. M.T.K. contributed to the neural recording and stimulation experiments and their analysis. R.P. developed the *in vivo* fluorescence detector and M.M. contributed to the *in vivo* fluorescence measurements and analysis. W.G. participated in immunostaining. C.R. designed and cloned the *hThy-1* and *hSyn* constructs. O.Y. provided the SFO viral vector. K.D. and K.V.S. supervised all aspects of the work.

### COMPETING FINANCIAL INTERESTS

The authors declare no competing financial interests.

Reprints and permissions information is available online at <http://npg.nature.com/reprintsandpermissions/>.

stimulation can be used for temporally more precise, but not cell type-specific, manipulations. Electrical stimulation also does not allow highly controlled inhibition and causes electrical interference that hampers the simultaneous electrical recording of neural signals from the same site. Optogenetics addresses these challenges by introducing into neurons light-sensitive proteins that regulate the ion conductance of the membrane. These proteins, encoded by microbial opsin genes, are derived from sources such as archaeobacteria and algae. They allow optical excitation<sup>2,3</sup> or inhibition<sup>4,5</sup> of specific neuron types based on their expression or projection patterns. Moreover, optogenetics allows simultaneous artifact-free electrical recording of action potentials<sup>6-8</sup>.

Optogenetics has been applied in a multitude of behavioral and electrophysiological studies in rodents<sup>6,9-13</sup>, and an initial study in rhesus monkeys has been successful<sup>14</sup>. However, three main challenges and constraints remain before optogenetic techniques are ready for broad application in non-human primate science, including neural prosthetics research<sup>15</sup>.

First, it is necessary to characterize the extent, efficiency, tolerance and pattern of opsin expression in non-human primate cortex to facilitate scientific interpretation of results, and to minimize potential risks. Viral vectors, promoters and opsins are the three relevant agents that need to be tested. In addition, the amount of laser power applied to the brain is of central interest as too much power can lead to thermal damage<sup>16-18</sup>. Second, the reliability of optogenetic stimulation and its effect on neural activity and behavior need to be tested to aid in the design of future experiments, and to maximize the chances of experimental success. Third, standard histological approaches, which are useful for analyzing expression patterns, can be performed only after completion of experiments. Experiments with behaviorally trained monkeys typically span months or years and result in extremely valuable experimental subjects. This makes standard histological evaluation less attractive. A method is needed that allows repeated *in vivo* fluorescence measurements in the non-human primate brain to determine expression levels and to find the opsin-expressing sites, which can be distant from the injection site because of axonal or trans-synaptic trafficking<sup>19</sup>.

Here we address these three challenges with a panel of optogenetic tools applied in rhesus macaques and tested with single-unit and local field potential electrophysiology. We also compare the effects of optical, electrical and combined opto-electronic stimulation in motor cortex on passive behavior, and show *in vivo* and *ex vivo* fluorescence measurements.

## RESULTS

We injected two monkeys at seven different sites with four different constructs (Fig. 1). These constructs included the membrane channel channelrhodopsin-2 (ChR2)<sup>2</sup>, which activates neurons when driven with blue light; the chloride pump enhanced *Natronomonas pharaonis* halorhodopsin (eNpHR2.0)<sup>5</sup>, which inhibits spiking when driven with yellow or green light; and a step-function opsin (SFO), which is a mutated version of channelrhodopsin (hChR2(C128S))<sup>20</sup> that puts neurons in a state of increased excitability for many seconds after a brief blue light pulse. This last effect can be reversed by a brief pulse of yellow light. Our promoter choices included two human promoters. *hSyn* has been implicated in the regulation of neurotransmitter release at synapses, particularly at glutamatergic and GABAergic synapses<sup>21</sup>. *hThy-1* is a gene for a cell-surface protein, and was originally discovered as a thymocyte antigen. It is also present on the axonal processes of neurons<sup>22</sup>. As primate-appropriate viral vectors, we chose adeno-associated virus (AAV) serotype 2 pseudotyped with serotype 5 (here referred to as AAV5). We injected 1  $\mu$ l of virus each millimeter from the cortical surface to a depth of 6–10 mm (normal to the brain surface), to test infections across all cortical layers and taking into account potential cortical folding. Monkey D was injected with AAV5-hSyn-ChR2-EYFP along a line through motor

and somatosensory cortex, as well as with AAV5-hThy-1-ChR2-EYFP and AAV5-hThy-1-eNpHR2.0-EYFP in motor cortex. Monkey B was injected with AAV5-hThy-1-ChR2-EYFP in somatosensory cortex. All AAV5 vectors had a titer of  $10^{12}$  particles per ml. We also injected one site in monkey B with a lentivirus carrying *hSyn-SFO-EYFP* in parietal cortex with a titer of  $10^9$ – $10^{10}$  particles per ml. Between weeks 5 and 12 after viral vector injection, we optically stimulated the injected sites while simultaneously recording neural activity. We also monitored potential effects of the optical stimulation on passive motor behavior, and compared and combined optical stimulation with electrical stimulation to explore effects on behavior. Five months after injection (monkey D) and four months after injection (monkey B), we assessed expression levels and patterns first by *in vivo* fluorescence measurement and subsequently with standard histological methods.

### Optogenetic inhibition

During the period between 5 and 12 weeks after injection of the eNpHR2.0 vector, we illuminated tissue with green (561 nm) or yellow (594 nm) light. Neurons responded with a rapid reduction in firing rate to pulse trains or continuous green light with latencies of 1–3 ms (Fig. 2a and Supplementary Fig. 1a, b). Power densities ranged from 3 mW mm<sup>-2</sup> to 255 mW mm<sup>-2</sup>, measured at the tip of the 200- $\mu$ m diameter fiber, which produced estimated power densities of 0.34 mW mm<sup>-2</sup> to 27 mW mm<sup>-2</sup> at the site of electrical recordings (the electrode tip typically led the fiber by 300  $\mu$ m; see Online Methods for calculation details and Supplementary Fig. 1c). For a quantitative analysis of how individual neurons responded to light, we performed a  $\chi^2$ -test (criterion  $P < 0.01$ ,  $\chi^2 = 3.8415$ , 1 degree of freedom) comparing baseline activity with activity during illumination. At the eNpHR2.0-expressing site we found that 38% (55/144) of all recorded single units and 22% (7/32) of all multi-units significantly changed their firing rate in response to green light (see Supplementary Table 1). Typically, responsive neurons decreased their firing rates (Fig. 2b and Supplementary Fig. 2a). Only fifteen cells responded with an increase in firing rate, presumably due to disinhibitory network effects (that is, optical inhibition of a neuron that inhibited the neuron under observation). To investigate further whether the firing rate increase was an indirect network effect or based on the stimulation of axons originating from ChR2-expressing sites we stimulated the eNpHR2.0-expressing site with blue light (Supplementary Figs. 2b and 3). We found that 17 units (single and multi-units) responded to blue light with an increase in firing rates (and 5 units with a decrease). There was a trend toward longer latencies (6–7 ms as opposed to the 2–3 ms latencies at ChR2-expressing sites; see below), which suggested that an indirect network effect was responsible, but short latency responses also occurred. Simultaneously with single-unit recordings, we measured local field potentials (LFPs). LFP deflections followed stimulation frequencies (Supplementary Fig. 4), and the polarity of LFP deflections caused by green or yellow light was positive with a negative rebound, as expected from the underlying ion flow. Blue light did not cause LFP modulations.

To test whether eNpHR2.0 expression had an effect on neuronal activity we compared baseline firing rates (that is, without optical stimulation) of light responsive and light unresponsive single units. Light responsive neurons did not differ significantly from light unresponsive neurons in their spontaneous activity (Wilcoxon rank-sum test;  $P = 0.3$ ; median light responsive neurons 2.8 Hz, median light unresponsive neurons 2.2 Hz; see Supplementary Table 2).

### Optogenetic excitation

We illuminated 127 and 53 single units from sites injected with *hSyn-ChR2* and *hThy-1-ChR2*, respectively, with blue (473 nm) light while simultaneously recording from them. To stimulate neurons while still being able to isolate them, we titrated the light intensities for

each individual neuron to a level that caused increased spiking without increasing the background activity to a level that would obscure the waveform of the neuron of interest. This resulted in a wide range of applied power densities ranging from 3 mW mm<sup>-2</sup> to 255 mW mm<sup>-2</sup> at the tip of the fiber (estimated power density of 0.25 mW mm<sup>-2</sup> to 20 mW mm<sup>-2</sup> at the electrical recording site; see Online Methods for calculation details). Neurons at ChR2-expressing sites responded strongly for all tested frequencies of light pulses (Fig. 3a, b and Supplementary Figs. 5 and 6). Neurons were able to follow 20-Hz stimulations (300 μs to 1 ms pulse width, energy densities of <0.25 μJ mm<sup>-2</sup> to 20 μJ mm<sup>-2</sup>) with average latencies of 3 ms. Spike frequencies increased during optical stimulation, whereas spike waveforms remained unaltered (Supplementary Fig. 6). With increasing stimulation frequency, the probability of each light pulse evoking a spike decreased. For higher frequencies (>50 Hz) and continuous stimulation we often observed an initial burst of activity followed by a reduction in firing rate (Supplementary Fig. 5c, d). In total, 50% (62/127) of all neurons recorded from sites injected with the ChR2-construct under the control of the *hSyn* promoter and 45% (24/53) from sites injected with ChR2-construct under the control of the *hThy-1* promoter responded significantly to blue light. A slightly higher percentage of multi-units passed the significance criterion (*hSyn*: 54/87 (62%); *hThy-1*: 14/23 (61%);  $\chi^2$ -test, criterion  $P < 0.01$ ,  $\chi^2 = 3.8415$ , 1 degree of freedom). The responses were mainly excitatory, with rare exceptions (three single units and two multi-units from *hSyn-ChR2* and two single units and two multi-units from *hThy-1-ChR2*-expressing sites showed overall suppression of spiking activity for at least one of the tested frequencies; Fig. 3c, d and Supplementary Fig. 7). Simultaneously measured LFPs revealed opposite polarities to LFPs evoked at the eNpHR2.0 injected site: deflections caused by blue light were negative with a positive rebound at sites expressing ChR2 (Supplementary Fig. 8). Again, this is as expected given the ionic currents that result from illumination of ChR2 and eNpHR2.0.

The light-responsive neurons did not differ significantly from light-unresponsive neurons in their spontaneous activity in areas injected with AAV5-hThy-1-ChR2-EYFP (Wilcoxon rank-sum test,  $P = 0.64$ ; median light-responsive neurons 6.5 Hz, median light-unresponsive neurons 7.9 Hz; see Supplementary Table 2). In areas injected with AAV5-hSyn-ChR2-EYFP, we found a slight reduction in baseline activity of light-responsive neurons ( $P = 0.04$ ; median light-responsive neurons 1.1 Hz, median light-unresponsive neurons 2.2 Hz).

### Effect of optical stimulation on passive movements

It has been reported that optical stimulation of ChR2 in the macaque frontal eye field does not cause overt movements<sup>14</sup>. To determine whether this is true for motor and somatosensory cortex, we monitored the contralateral arm and hand during optical stimulation in both monkeys (Fig. 4). We analyzed 18 stimulation sessions for monkey D and 8 sessions for monkey B. Despite the strong neuronal responses to light, which we recorded simultaneously at the same site with optrodes, we saw no effect on spontaneous motor behavior (the resting arm and hand did not twitch or move during optical stimulation). This was the case even at sites where standard intracortical electrical stimulation reliably caused arm and hand movements.

As a potentially more sensitive assay, we also tested whether optical stimulation could modulate the effect of electrical stimulation in motor cortex in monkey D. We therefore performed electrical stimulation using current levels just barely above threshold with and without simultaneous optical stimulation (see Online Methods for stimulation parameters). We found no increase (or decrease) in electrically evoked hand deflections with the addition of blue light stimulation at ChR2-injected sites (Fig. 4a). Similarly, inhibition with yellow light at an eNpHR2.0 site did not result in a decrease (or increase) in movements induced by electrical stimulation (Fig. 4b). Finally, we attempted to 'prime' electrical stimulation trains

with preceding optical stimulation. Again, this did not seem to influence the magnitude of hand movements. In summary, despite the fact that stimulation with blue light increased neuronal activity by up to two orders of magnitude relative to baseline activity (Fig. 3c, d) and that hand deflections were evoked by electrical stimulations at the same site, we did not observe an effect of optical stimulation on passive hand movements. This suggests that there is a mechanistic difference between optical and electrical stimulation. In addition to the hand, we monitored the rest of the monkeys' bodies during optical stimulation. Stimulation did not result in any reproducible change in body posture or any seizure-like behavior.

### Bistable optogenetic excitation

We also recorded activity from 12 single units and 17 multi-units from monkey B at sites injected with Lenti-hSyn-ChR2(C128S)-EYFP. On the basis of results in rodents, we expected to see long-lasting increases in neural activity after brief pulses of blue light. This effect has been described to be reversible by yellow light pulses<sup>20</sup>. Owing to the cumulative nature of SFO activity, we further expected that short, low-intensity light pulses would gradually increase the activity of the expressing neurons because of increased depolarization with repeated light pulses.

Four single units (33%) and six multi-units (26%) showed the expected long-lasting response to a 10-ms blue light pulse. Although a single 10-ms pulse of blue light (3–255 mW mm<sup>-2</sup> at the tip of the fiber) typically evoked 1–3 spikes in light-responsive neurons at ChR2-expressing sites, a single 10-ms pulse of blue light of the same intensity range caused neurons at the SFO-expressing site to increase their firing rates for several seconds (Fig. 5a–c and Supplementary Fig. 9a). On average, 355 spikes were evoked by a single pulse, which makes the SFO more than 100 times as 'responsive' as ChR2. A 500-ms illumination with yellow light reversed the effect, resulting in abrupt return of the firing rate to the baseline (Fig. 5d). Repeated pulsing of blue light (10 ms pulse width, 2 s pulse interval, average power density of 0.1 mW mm<sup>-2</sup>; see Online Methods for calculation details) caused a stepwise increase in firing rate until it reached a plateau after six light pulses (Fig. 5e and Supplementary Fig. 9b).

### *In vivo* fluorescence detection of opsin expression

For non-human primate studies, which typically take years, it would be desirable to determine expression *in vivo* while experiments are ongoing. This would allow researchers to monitor expression over the weeks after the injections and to determine the ideal time to starting recordings. Importantly, it would allow independent verification of viral vector delivery and opsin-EYFP expression separately from the electrophysiological functionality of the proteins encoded by the opsin genes. We developed and applied a new fluorescence detection device to achieve this goal, which for optimal versatility and minimal tissue damage uses a single fiber optic cable both to deliver source light and to detect the emitted fluorescent light (from enhanced yellow fluorescent protein, EYFP; Fig. 6a). In this design the same fiber can be used to deliver light for neural modulation (when used for optogenetic experiments) and to deliver light for fluorescence excitation (when used for *in vivo* fluorescence measurements). The fiber delivers excitation light pulses to the region of interest and guides a sample of the corresponding emission signal back to a sensitive low-noise detector. Parallel to this first photodetector, a second detector is used to eliminate the effect of input light fluctuations, imperfection of the optical filters, self-fluorescence at the tip of the fiber and random back-reflection of the excitation or stimulation light when the operator moves the fiber up and down within tissue. We used a set of optical fiber splitters to combine the input light, which was generated by numerous light sources, and to distribute the emission signal in the system. To further improve the signal-to-noise ratio we applied a combination of patterned pulses and a software-based time-lens filter (see Online Methods).



Compared with traditional dichroic-based setups<sup>23</sup>, the new system is smaller and more mobile, is more robust and requires minimal alignment. The device was connected to an optrode that collected fluorescence measurements while moving dorsoventrally.

We observed fluorescence increases as the fiber entered cortex, consistent with the fluorescence levels across the injected area as confirmed by subsequent confocal microscopy of frozen brain slices (Fig. 6b). The *in vivo* measured signal increased 1–2 mm below the cortical surface, as expected because the device integrates across the volume in front of the fiber. In fixed slices, we measured fluorescence from an angle perpendicular to the brain surface. This led to measurements that reflected more closely the intensity profile in the fluorescence image. As we conducted the *in vivo* fluorescence measurements with the same optrode that was used for optical stimulation, simultaneous electrical recordings were possible. The *in vivo* fluorescence measurements correlated with the neural responses to light stimulation (Fig. 6c). Only at depths that showed an increased fluorescence level did we find neurons that responded to the optical stimulation. To confirm that fluorescence caused by the opsin-EYFP expression can be discriminated from autofluorescence in the primate brain, we conducted measurements in the perfused brain of monkey B. We compared measurements from a region that expressed opsin-EYFP with measurements from visual cortex of the contralateral hemisphere, an area that is not known to receive projections from somatosensory cortex of the other hemisphere<sup>24</sup>. In contrast to quantified fluorescence at the injected site, there was no significant change in the control region of visual cortex (Supplementary Fig. 10).

To test whether expression can be tracked over time we injected rats with AAV5-hSyn-ChR2-EYFP in motor cortex and hippocampus (Fig. 6d). Over the course of 35 days the fluorescence signal increased exponentially (Fig. 6e). After this period the fluorescence increase slowed down, giving the overall time-expression curve a sigmoidal shape. Control rats that were implanted with a fiber but did not receive a virus injection did not show any difference in fluorescence signal. To test whether expression in projecting fibers can be detected by the *in vivo* fluorescence detector we measured fluorescence in the hippocampus contralateral to the injected hemisphere over the same time span. We found that fluorescence increased steadily but that this increase lagged behind that seen at the injected sites, and that fluorescence was much weaker than at injected sites, as expected because we were measuring only projecting fibers.

### Histological evaluation of opsin expression

At the end of the experiment, we used standard histological techniques to determine expression patterns. Both promoters, *hThy-1* and *hSyn*, resulted in strong local expression in cell bodies, dendrites and axons as well as in fibers that projected to subcortical structures (see arching green lines in Fig. 7a). The *hThy-1* promoter led to particularly strong labeling of local dendrites, whereas *hSyn* caused particularly pronounced expression in axons that projected to other cortical areas (Fig. 7b). Within cortex, we found labeled fibers more than 5 cm away from injections (for example, fibers following the projection from motor cortex to supplementary motor cortex (SMA)<sup>25</sup>), indicating that cortico-cortical projections could be targeted with these constructs. To evaluate the efficiency of the different constructs and viral vectors we calculated the ratio of expressing cells in injected and non-injected sites (Fig. 7c, d, Supplementary Tables 3–6 and Supplementary Fig. 11). We found that 43.9% (1174/2673) of all neurons showed expression within a 3-mm circle centered on the AAV5-hSyn-ChR2-EYFP injection. In layers 4–5 the expression levels were as high as 77% (154/199). Directly adjacent to the strongly expressing area, the expression levels dropped to 0.6% (6/1028), producing a sharp border between expressing and non-expressing tissue. When moving further away from the injection site (3 mm and 11.5 mm from the center of the injection site) we encountered only one expressing neuron even though these areas

(especially the 11.5 mm distant SMA) showed strong expression in fibers. When we used the same promoter but in a lentivirus (Lenti-hSyn-SFO-EYFP) and at a lower titer, the efficiency was lower (24.7% transfected neurons or 375/1520 averaged across all layers, and 38% or 92/240 at layers 4 and 5). At the center of injections, both constructs under the control of the *hThy-1*-promoter showed similar expression levels as did AAV5-hSyn-ChR2-EYFP (AAV5-hThy-1-ChR2-EYFP: 42.9% or 725/1691 averaged across all layers and 67.8% or 162/239 at layers 4 and 5; AAV5-hThy-1-eNpHR2.0-EYFP: 40.0% or 448/1121 averaged across all layers and 64.6% or 95/147 in layers 4 and 5). In comparison to AAV5-hSyn-ChR2-EYFP, the drop-off of EYFP-expressing cells was more gradual under the control of the *hThy-1*-promoter (AAV5-hThy-1-ChR2-EYFP: 11.5% or 145/1266 at 1.1 mm from injection center; AAV5-hThy-1-eNpHR2.0-EYFP: 22.3% or 231/1035 at 1.1 mm from injection center). The upper layers of cortex did not express the opsins, regardless of promoter, opsin type and viral vector. To test whether this finding was specific to the vicinity of the cortical surface, we analyzed the expression patterns in cortical sulci. There, we observed the same lack of expression in upper layers (Fig. 7c, d, Lenti-hSyn-SFO-EYFP, derived from the sulcus).

In very rare cases (0.08% or 1/1233) we encountered labeled neurons in non-injected areas. This effect seems most likely to be caused by retrograde transport, a mechanism that can occur with specific AAV serotypes<sup>26</sup>. In summary, this injection scheme, which separated the sites of injections by 4 mm on the surface of cortex, led to robust and non-overlapping expression patches between layers 4 and 6 (however, labeled axons are likely to reach over and cross into neighboring injected areas).

Both the *hSyn* and *hThy-1* promoters are expected to drive expression and produce functional opsins in both excitatory and inhibitory neurons. To determine the proportions of neurons of each type that expressed EYFP, we immunostained cortical slices with antibodies against the excitatory neuron-specific marker  $\alpha$ -CaMKII<sup>27</sup> and the inhibitory neuron-specific neurotransmitter GABA<sup>28</sup>. As expected, owing to the known smaller proportion of inhibitory neurons in cortex<sup>29</sup>, we found a smaller percentage of EYFP-expressing cells that were also labeled with GABA than were also labeled with  $\alpha$ -CaMKII (Supplementary Fig. 12 and Supplementary Table 7). To ensure that the virally expressed proteins were functional in both cell types, we used waveform shape to identify putative excitatory and inhibitory neurons during electrophysiological recordings<sup>30,31</sup> (though note that this technique can produce misclassifications<sup>32</sup>). We found that similar proportions of both cell types were light-sensitive (Supplementary Fig. 13 and Supplementary Table 8).

To investigate long-term effects of the virus infection and opsin expression in the brain we analyzed the status of EYFP-opsin expressing neurons with the nuclear marker 4',6-diamidino-2-phenylindole (DAPI), the neuron-specific nuclear marker (NeuN)<sup>33</sup> and the astro-cyte-specific marker glial fibrillary acidic protein (GFAP)<sup>34</sup>. Cell nuclei of infected cells appeared to be intact and the morphology of infected neurons appeared normal 4–5 months after injections with high-titer viruses (Fig. 8). Expression was exclusively restricted to neurons and we found no infected astroglia (Supplementary Fig. 11d). All of the neurons that expressed opsin and EYFP also expressed NeuN (AAV5-hSyn-ChR2-EYFP, 121/121 cells; AAV5-hThy-1-ChR2-EYFP, 119/119; AAV5-hThy-1-eNpHR2.0-EYFP, 111/111; Lenti-hSyn-SFO-EYFP, 120/120) but none co-expressed GFAP (0/121, 0/119, 0/111 and 0/120, respectively). In areas that received projections, expression was limited to projecting axons (Fig. 7b). Whereas neurons looked healthy in general, we found aggregations of ChR2-EYFP in dendrites in areas injected with AAV5-hSyn-ChR2-EYFP (Fig. 8a, right), which seem to be a sign of overexpression. However, neurons with aggregates had normal cell shapes and no abnormal staining. Further from the center of the injections the aggregations vanished. We found fewer of these aggregations with the same construct under

control of the *hThy-1* promoter (Fig. 8b). The same promoter *hSyn* controlling *SFO-EYFP* expression delivered with a lower titer lentiviral vector also produced fewer aggregations (Fig. 8c). Aggregations were completely absent at the site injected with AAV5-*hThy-1*-eNpHR2.0-EYFP (Fig. 8d).

## DISCUSSION

In this study we sought to develop and test optogenetic tools specifically for the needs of researchers using non-human primates. In the course of these efforts, we assessed the safety and efficacy of two different viral vectors, two primate-specific promoters and three different opsins on an electrophysiological and histological level. Furthermore, we compared and combined optical and electrical stimulation in motor cortex to evaluate its impact on passive movements. We also introduced technology for *in vivo* tracking of expression of fluorescent proteins in the living primate and rodent brain, which is essential for evaluating expression, guiding recordings and improving experimental yield. With the combination of viral vectors, promoters and opsins reported here and in previous work, reliable optogenetic excitation and inhibition of neural activity in non-human primates seems to be possible. Below we discuss the merits and current limitations of this technique to advance the design of future non-human primate neuroscience and neural prosthetic experiments.

### Safety of optogenetics in non-human primates

We found that AAV5, which is safe for use in non-human primates<sup>35,36</sup>, can be used as a safe and effective viral vector for delivering opsins into the brains of non-human primates. AAVs are known to be tolerated by the human immune system<sup>37</sup>. Although AAV2 has been successfully used for gene therapies<sup>38</sup>, AAV5 might be preferable because it shows very low neutralizing factor seroprevalence in humans (3.2% as opposed to 59% for AAV2)<sup>39</sup> and diffuses more readily in brain tissue<sup>40</sup>. To increase efficacy we also introduced here a set of primate promoters (both *hSyn* and *hThy-1* are derived from the human genome) that are suitable for balanced expression in excitatory and inhibitory primate neurons. Histological workup confirmed high and well-tolerated neuron-specific expression in somata and projections under both promoters. However, we noted apparent ChR2-EYFP aggregations with *hSyn* and to a much lesser degree with the *hThy-1* promoter. Such aggregations may be linked to overexpression and could have an effect on cell health. The appearance of cell bodies and nuclei did not give indications of cell deterioration but we cannot rule out the possibility that these aggregates have negative effects on the cells' metabolism. We used electrical recordings to confirm that opsin-expressing neurons were functional (they produced action potentials) both with and without light stimulation. The slightly lower baseline firing rate of light-responsive neurons in sites injected with AAV5-*hSyn*-ChR2-EYFP as compared to light-unresponsive units might indicate an unhealthy trend of neuron activity which might be coupled to the aggregate formation. Aggregation could be reduced or completely avoided by using a less strong promoter (like *hThy-1*), by using a lentiviral vector instead of AAV5 (or a low virus titer instead of a high virus titer), or by enhancing trafficking as successfully implemented in eNpHR2.0 (ref. 5). With our *in vivo* fluorescence device we have found that expression increases exponentially over the course of 5–7 weeks, after which fluorescence approached what might be a saturation level. As the histological studies were done 1–2 months past the 7-week time point we believe that the observed expression patterns were probably close to the maximum.

In addition to potential opsin overexpression, the recording and stimulation equipment itself can cause tissue damage. Although we were able to successfully record for more than 20 sessions from each injected site with the current optrode design, we noted that cortical damage was caused by the currently used optrodes. We believe that this damage could be



substantially reduced by switching from the ‘two-tip’ design (fiber + electrode) to a ‘co-axial’ optrode with a single, smaller tip<sup>8</sup>. Another safety issue is phototoxicity, a phenomenon known from live cell imaging, where illuminating a fluorescent molecule causes the selective death of the cells that express it<sup>41</sup>. That we were able to optically stimulate and record from cells over the course of over 60 trials, and to record neural activity from the same site after 20 stimulation and recording sessions, suggests that phototoxicity is not a safety concern for optogenetic manipulations with the laser power densities used here.

Finally, the regularity of optical ChR2 stimulations raises the issue of evoking seizures. We therefore closely monitored the monkeys during optical stimulations. We never observed seizure-like behavior.

### **Efficacy of optogenetics in non-human primates**

We found that 38–50% of all neurons recorded at AAV5-injected sites were light-responsive, in accordance with the histological finding that 40–43% of neurons expressed the construct. This level of expression might seem low but is comparable with other (non-optogenetic) virus characterization studies<sup>40,42</sup>. There are substantial differences between the different AAV serotypes<sup>40</sup> and virus chimerae promise higher efficacy<sup>43</sup>.

Unexpectedly, we did not find cells expressing opsin and EYFP in layers 1 and 2/3 with any of the tested constructs. Expression was almost exclusively restricted to layers 4–6. We found the same reduction of expression in upper cortical layers in sulci, arguing against any surface-related explanations (for example, virus escape to the surface). Viral tropism and layer-specific promoter read-out alone seem unlikely to be the reason for this expression pattern because AAVs and lentiviruses express in all cortical layers<sup>42</sup>. However, the specific combination of promoter, viral vector and titer might have caused the layer specificity. Although the observed expression pattern is surprising it also offers opportunities, by virtue of allowing deep layer-specific stimulation.

In the horizontal dimension perpendicular to the injection track, expression occurred only in a defined diameter of about 1.5–2 mm around the injection track. However, transport of the opsin to axons can lead to expression many millimeters away from the injected area, thus allowing projection stimulation<sup>19</sup>. The neuron activation caused by blue light in an eNpHR2.0-expressing site that we encountered was probably caused by such stimulation of axons originating from ChR2-expressing sites. For non-human primate studies, in which suitable promoter fragments for specificity are limited, axonal targeting offers a promoter-independent targeting possibility<sup>19,44,45</sup>.

We demonstrated efficacy and functionality of optogenetic control in the expressing neurons by optical stimulation paired with electrical recordings across months after injections. As expected from the channel kinetics, SFO channels only needed a brief pulse of blue light to be activated for many seconds whereas ChR2-expressing neurons responded with only one spike per light pulse. For ChR2, low-frequency stimulation (<50 Hz) was most reliable in causing action potentials. We sometimes encountered effects opposite to the expected directions (blue light causing inhibition at ChR2-expressing sites and green light causing excitation at eNpHR2.0 expressing sites). This was probably caused by an indirect network effect arising from non-expressing neurons receiving increased or decreased inhibitory input from opsin-expressing neurons. However, the overall network activity, as measured with LFPs, showed a strong effect that was in accordance with the expected ion flow. At eNpHR2.0-expressing sites illuminated with yellow light, Cl<sup>-</sup> is pumped into neurons, causing a relative increase in positive charges (positive deflections of the LFP signal) in the extracellular milieu. At ChR2-expressing sites, Na<sup>+</sup> flows into the cells when blue light is present causing a relative decrease in positive charges (negative deflections of the LFP

signal) in the extra-cellular milieu. This is consistent with population-wide inhibition of neural activity at eNpHR2.0-injected sites and population-wide excitation of neural activity at ChR2-injected sites.

We found that optical stimulation in cortical motor and premotor areas did not evoke movements. This finding contrasts with the large effect of optical stimulation on neuronal activity and the ability to evoke movements by electrical stimulations with an electrode in close proximity to the optical fiber tip. Hence, it would appear that optical stimulation did not perturb the system in some way that electrical stimulation does. It is possible that the observed 40–50% of channel-expressing neurons is not enough to yield a behavioral effect. Employing more effective virus serotypes and chimerae could be a solution<sup>43</sup>. However, there are other possibilities. First, the observed specificity for deeper layers is contrasted by electrical stimulation, which is likely to affect all cortical layers. Second, the region of stimulation might have been too small to cause overt movement. Whereas electrical stimulation can affect neurons several millimeters away from the stimulating electrode<sup>46</sup> by activating distant non-targeted cells that happen to have axonal projections or collaterals near the electrode, optical stimulation only affects approximately 1 mm<sup>3</sup> around the tip of the fiber<sup>10</sup> owing to the local expression of light-sensitive channels and the limited spread of light. Although this small volume seems to be enough to evoke movements in rodents<sup>6</sup>, the rhesus monkey brain is approximately 250 times larger and might therefore require a larger volume of activated tissue. The introduction of larger fiber diameters and larger numerical apertures for broader light cones, or multiple optical fibers for multi-site stimulation, could be beneficial. However, this will inevitably cause more cortical damage. Engineered opsin genes designed for enhanced light sensitivity, photocurrent size and red-shifted action spectra (allowing greater light spread in tissue)<sup>19</sup> are therefore preferable options to improve the toolbox. Third, it is also conceivable that the frequencies of our optical stimulation were not high enough. Electrical stimulation uses pulse trains at several hundred Hz (for example, 300–350 Hz), and it is possible that specific neuron classes follow these high electrical stimulation frequencies. ChR2-expressing neurons, meanwhile, could only follow lower optical stimulation frequencies reliably, with 20–50 Hz being the maximum for reliably evoking spikes. Future experiments using opsins with faster kinetics such as ChETA<sup>47</sup> might allow this possibility to be explored. Fourth, compensation dynamics might have masked the effect of the optical stimulation. Fifth, it has been shown that neural activity in primary motor cortex and premotor cortex can increase without causing movement or even EMG activity<sup>48</sup>. Therefore it is conceivable that we did not activate the right neuron populations in the exact way necessary to generate muscle activity. Finally, we focused on passively evoked movements in this study. More sensitive measures of behavior might be required, such as optical stimulation while animals are actively involved in a task. In those settings, electrical subthreshold stimulation (stimulation that does not evoke any overt movement) has been shown to influence behavior<sup>49</sup>. A similar protocol might therefore be more likely to reveal an effect of optical stimulation.

The aim of this study was to help to enable safe, reliable and effective experiments using tools designed specifically for non-human primates. We believe that the characterization of optogenetics is an ongoing process. However, optogenetic gain- and loss-of-function experiments, such as those described here, might allow a sequence of electrophysiology studies similar to classic pharmacological and electrical microstimulation experiments, with increased temporal resolution and cell-type specificity.

## METHODS

Methods and any associated references are available in the online version of the paper at <http://www.nature.com/natureneuroscience/>.

## Supplementary Material

Refer to Web version on PubMed Central for supplementary material.

## Acknowledgments

We thank M. Vessal and A. Lilak for technical assistance during perfusions, M. Churchland for technical support during surgeries and technical discussions, S. Ryu for surgical assistance, M. Risch for veterinary care, D. Haven for technical support, S. Eisensee for administrative assistance, I. Witten for advice and members of the Deisseroth and Shenoy laboratories for discussions. I.D. is supported by a Human Frontier Science Program fellowship and a German Academic Exchange Service Award, M.T.K. by a National Science Foundation graduate fellowship, M.M. by Bio-X and a Stanford Graduate Fellowship and R.P. by a Stanford University Dean's Postdoctoral Fellowship Award. W.G. is supported by a Stanford Graduate Fellowship. O.Y. is supported by a Human Frontier Science Program fellowship. K.D. is supported by the William M. Keck Foundation, the Snyder Foundation, the Albert Yu and Mary Bechmann Foundation, the Wallace Coulter Foundation, the California Institute for Regenerative Medicine, the McKnight Foundation, the Esther A. and Joseph Klingenstein Fund, the National Science Foundation, the National Institute of Mental Health, the National Institute on Drug Abuse and a US National Institutes of Health Director's Pioneer Award. K.V.S. is supported by a Burroughs Wellcome Fund Career Award in the Biomedical Sciences, US National Institutes of Health–National Institute of Neurological Disorders and Stroke grant CRCNS R01-NS054283 and a US National Institutes of Health Director's Pioneer Award (1DP1OD006409). K.D. and K.V.S. are supported by Defense Advanced Research Projects Agency Reorganization and Plasticity to Accelerate Injury Recovery (N66001-10-C-2010).

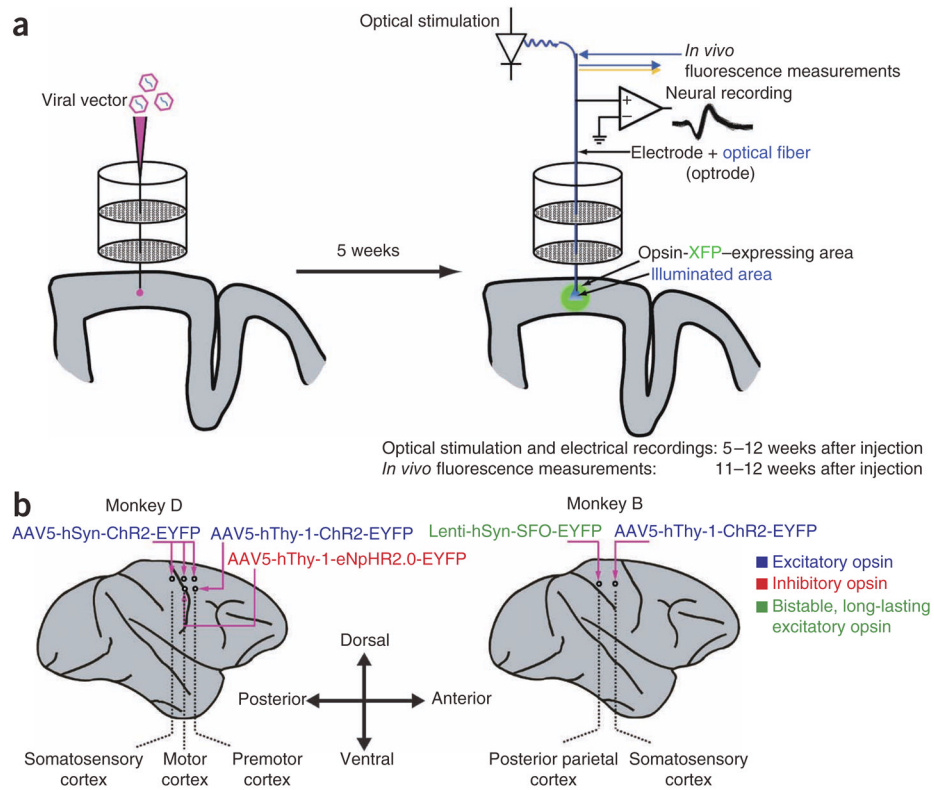
## References

- Hikosaka O, Wurtz RH. Effects on eye movements of a GABA agonist and antagonist injected into monkey superior colliculus. *Brain Res.* 1983; 272:368–372. [PubMed: 6311342]
- Boyden ES, Zhang F, Bamberg E, Nagel G, Deisseroth K. Millisecond-timescale, genetically targeted optical control of neural activity. *Nat Neurosci.* 2005; 8:1263–1268. [PubMed: 16116447]
- Zhang F, Wang LP, Boyden ES, Deisseroth K. Channelrhodopsin-2 and optical control of excitable cells. *Nat Methods.* 2006; 3:785–792. [PubMed: 16990810]
- Zhang F, et al. Multimodal fast optical interrogation of neural circuitry. *Nature.* 2007; 446:633–639. [PubMed: 17410168]
- Gradinaru V, Thompson KR, Deisseroth K. eNpHR: a *Natronomonas* halorhodopsin enhanced for optogenetic applications. *Brain Cell Biol.* 2008; 36:129–139. [PubMed: 18677566]
- Gradinaru V, et al. Targeting and readout strategies for fast optical neural control *in vitro* and *in vivo*. *J Neurosci.* 2007; 27:14231–14238. [PubMed: 18160630]
- Zhang F, et al. Optogenetic interrogation of neural circuits: technology for probing mammalian brain structures. *Nat Protoc.* 2010; 5:439–456. [PubMed: 20203662]
- Zhang J, et al. Integrated device for optical stimulation and spatiotemporal electrical recording of neural activity in light-sensitized brain tissue. *J Neural Eng.* 2009; 6:055007. [PubMed: 19721185]
- Adamantidis AR, Zhang F, Aravanis AM, Deisseroth K, de Lecea L. Neural substrates of awakening probed with optogenetic control of hypocretin neurons. *Nature.* 2007; 450:420–424. [PubMed: 17943086]
- Aravanis AM, et al. An optical neural interface: *in vivo* control of rodent motor cortex with integrated fiberoptic and optogenetic technology. *J Neural Eng.* 2007; 4:S143–S156. [PubMed: 17873414]
- Gradinaru V, Mogri M, Thompson KR, Henderson JM, Deisseroth K. Optical deconstruction of parkinsonian neural circuitry. *Science.* 2009; 324:354–359. [PubMed: 19299587]
- Airan RD, Thompson KR, Fenno LE, Bernstein H, Deisseroth K. Temporally precise *in vivo* control of intracellular signaling. *Nature.* 2009; 458:1025–1029. [PubMed: 19295515]
- Tsai HC, et al. Phasic firing in dopaminergic neurons is sufficient for behavioral conditioning. *Science.* 2009; 324:1080–1084. [PubMed: 19389999]
- Han X, et al. Millisecond-timescale optical control of neural dynamics in the nonhuman primate brain. *Neuron.* 2009; 62:191–198. [PubMed: 19409264]
- Gilja V, et al. Challenges and opportunities for next-generation intra-cortically based neural prostheses. *IEEE Trans Biomed Eng.* in the press.

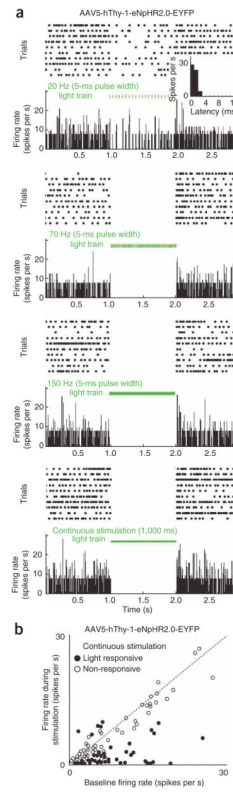
16. Kim S, Tathireddy P, Normann RA, Solzbacher F. Thermal impact of an active 3-D microelectrode array implanted in the brain. *IEEE Trans Neural Syst Rehabil Eng.* 2007; 15:493–501. [PubMed: 18198706]
17. Lee JH, et al. Global and local fMRI signals driven by neurons defined optogenetically by type and wiring. *Nature.* 2010; 465:788–792. [PubMed: 20473285]
18. Cardin JA, et al. Targeted optogenetic stimulation and recording of neurons *in vivo* using cell type-specific expression of Channelrhodopsin-2. *Nat Protoc.* 2010; 5:247–254. [PubMed: 20134425]
19. Gradinaru V, et al. Molecular and cellular approaches for diversifying and extending optogenetics. *Cell.* 2010; 141:154–165. [PubMed: 20303157]
20. Berndt A, Yizhar O, Gunaydin LA, Hegemann P, Deisseroth K. Bi-stable neural state switches. *Nat Neurosci.* 2009; 12:229–234. [PubMed: 19079251]
21. Bogen IL, Haug KH, Roberg B, Fonnum F, Walaas SI. The importance of synapsin I and II for neurotransmitter levels and vesicular storage in cholinergic, glutamatergic and GABAergic nerve terminals. *Neurochem Int.* 2009; 55:13–21. [PubMed: 19428802]
22. Caroni P. Overexpression of growth-associated proteins in the neurons of adult transgenic mice. *J Neurosci Methods.* 1997; 71:3–9. [PubMed: 9125370]
23. Adelsberger H, Garaschuk O, Konnerth A. Cortical calcium waves in resting newborn mice. *Nat Neurosci.* 2005; 8:988–990. [PubMed: 16007081]
24. Disbrow E, Litinas E, Recanzone GH, Padberg J, Krubitzer L. Cortical connections of the second somatosensory area and the parietal ventral area in macaque monkeys. *J Comp Neurol.* 2003; 462:382–399. [PubMed: 12811808]
25. Leichnetz GR. Afferent and efferent connections of the dorsolateral precentral gyrus (area 4, hand/arm region) in the macaque monkey, with comparisons to area 8. *J Comp Neurol.* 1986; 254:460–492. [PubMed: 3805358]
26. Burger C, et al. Recombinant AAV viral vectors pseudotyped with viral capsids from serotypes 1, 2 and 5 display differential efficiency and cell tropism after delivery to different regions of the central nervous system. *Mol Ther.* 2004; 10:302–317. [PubMed: 15294177]
27. Jones EG, Huntley GW, Benson DL. Alpha calcium/calmodulin-dependent protein kinase II selectively expressed in a subpopulation of excitatory neurons in monkey sensory-motor cortex: comparison with GAD-67 expression. *J Neurosci.* 1994; 14:611–629. [PubMed: 8301355]
28. Houser CR, Hendry SH, Jones EG, Vaughn JE. Morphological diversity of immunocytochemically identified GABA neurons in the monkey sensory-motor cortex. *J Neurocytol.* 1983; 12:617–638. [PubMed: 6352867]
29. Markram H, et al. Interneurons of the neocortical inhibitory system. *Nat Rev Neurosci.* 2004; 5:793–807. [PubMed: 15378039]
30. Diester I, Nieder A. Complementary contributions of prefrontal neuron classes in abstract numerical categorization. *J Neurosci.* 2008; 28:7737–7747. [PubMed: 18667606]
31. Kaufman MT, et al. Roles of monkey premotor neuron classes in movement preparation and execution. *J Neurophysiol.* 2010; 104:799–810. [PubMed: 20538784]
32. Calvin WH, Sybert GW. Fast and slow pyramidal tract neurons: an intracellular analysis of their contrasting repetitive firing properties in the cat. *J Neurophysiol.* 1976; 39:420–434. [PubMed: 1255231]
33. Mullen RJ, Buck CR, Smith AM. NeuN, a neuronal specific nuclear protein in vertebrates. *Development.* 1992; 116:201–211. [PubMed: 1483388]
34. McLendon RE, Bigner DD. Immunohistochemistry of the glial fibrillary acidic protein: basic and applied considerations. *Brain Pathol.* 1994; 4:221–228. [PubMed: 7952263]
35. Colle MA, et al. Efficient intracerebral delivery of AAV5 vector encoding human ARSA in non-human primate. *Hum Mol Genet.* 2010; 19:147–158. [PubMed: 19837699]
36. Dodiya HB, et al. Differential transduction following basal ganglia administration of distinct pseudotyped AAV capsid serotypes in nonhuman primates. *Mol Ther.* 2010; 18:579–587. [PubMed: 19773746]
37. Kaplitt MG, et al. Safety and tolerability of gene therapy with an adeno-associated virus (AAV) borne *GAD* gene for Parkinson's disease: an open label, phase I trial. *Lancet.* 2007; 369:2097–2105. [PubMed: 17586305]

38. Christine CW, et al. Safety and tolerability of putaminal AADC gene therapy for Parkinson disease. *Neurology*. 2009; 73:1662–1669. [PubMed: 19828868]
39. Boutin S, et al. Prevalence of serum IgG and neutralizing factors against adeno-associated virus types 1, 2, 5, 6, 8 and 9 in the healthy population: implications for gene therapy using AAV vectors. *Hum Gene Ther*. 2010; 21:704–712. [PubMed: 20095819]
40. McFarland NR, Lee JS, Hyman BT, McLean PJ. Comparison of transduction efficiency of recombinant AAV serotypes 1, 2, 5, and 8 in the rat nigrostriatal system. *J Neurochem*. 2009; 109:838–845. [PubMed: 19250335]
41. Frigault MM, Lacoste J, Swift JL, Brown CM. Live-cell microscopy—tips and tools. *J Cell Sci*. 2009; 122:753–767. [PubMed: 19261845]
42. Nathanson JL, Yanagawa Y, Obata K, Callaway EM. Preferential labeling of inhibitory and excitatory cortical neurons by endogenous tropism of adeno-associated virus and lentivirus vectors. *Neuroscience*. 2009; 161:441–450. [PubMed: 19318117]
43. Grimm D, et al. *In vitro* and *in vivo* gene therapy vector evolution via multispecies interbreeding and retargeting of adeno-associated viruses. *J Virol*. 2008; 82:5887–5911. [PubMed: 18400866]
44. Gordon T, et al. Accelerating axon growth to overcome limitations in functional recovery after peripheral nerve injury. *Neurosurgery*. 2009; 65:A132–A144. [PubMed: 19927058]
45. Chen CH, et al. Role of PKA in the anti-Thy-1 antibody-induced neurite outgrowth of dorsal root ganglionic neurons. *J Cell Biochem*. 2007; 101:566–575. [PubMed: 17177293]
46. Histed MH, Bonin V, Reid RC. Direct activation of sparse, distributed populations of cortical neurons by electrical microstimulation. *Neuron*. 2009; 63:508–522. [PubMed: 19709632]
47. Gunaydin LA, et al. Ultrafast optogenetic control. *Nat Neurosci*. 2010; 13:387–392. [PubMed: 20081849]
48. Taylor DM, Tillery SI, Schwartz AB. Direct cortical control of 3D neuroprosthetic devices. *Science*. 2002; 296:1829–1832. [PubMed: 12052948]
49. Churchland MM, Shenoy KV. Delay of movement caused by disruption of cortical preparatory activity. *J Neurophysiol*. 2007; 97:348–359. [PubMed: 17005608]



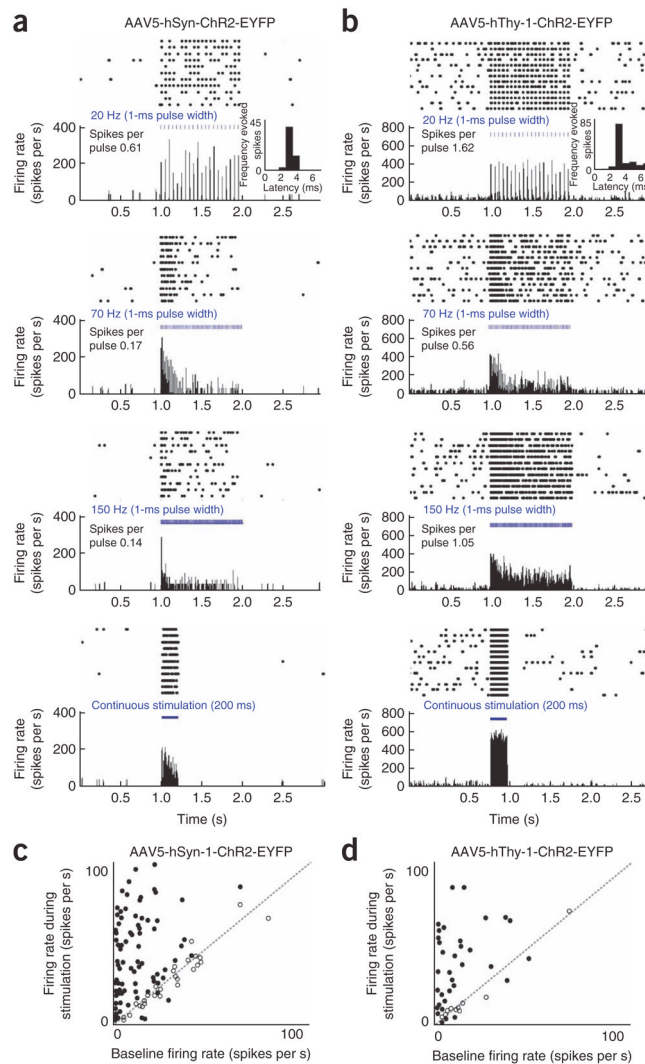
**Figure 1.**

Schematic overview of preparation. **(a)** Left, injection device; right, stimulation, recording and *in vivo* fluorescence detector outline. A standard recording grid guided an injection needle to the desired location. Small quantities (1  $\mu$ l) of viral vectors carrying the opsin-fluorophore fusion gene were injected at different depths and sites in cortex. Starting 5 weeks after injections we stimulated the injected sites optically and simultaneously recorded electrical neural activity using a combination of an optical fiber and an electrode (optrode) guided by the same grid as used for the injections. During the last week of the experiment we also measured *in vivo* fluorescence. **(b)** Injection sites and viral vectors in monkeys D and B. Monkey D was injected at five different sites with three different constructs. Along a line through motor (AP 16 mm, ML 6 mm and AP 11 mm, ML 6 mm) and somatosensory cortex (AP 7 mm, ML 6 mm) we injected AAV5-hSyn-ChR2-EYFP. More laterally, we injected at two different sites in motor cortex, AAV5-hThy-1-eNpHR2.0-EYFP and AAV5-hThy-1-ChR2-EYFP (AP 11 mm, ML 10 mm and AP 16 mm, ML 10 mm, respectively). Monkey B was injected with AAV5-hThy-1-ChR2-EYFP in somatosensory cortex (AP 6 mm, ML 14 mm) and with Lenti-hSyn-SFO-EYFP in parietal cortex (AP 2 mm, ML 14 mm).



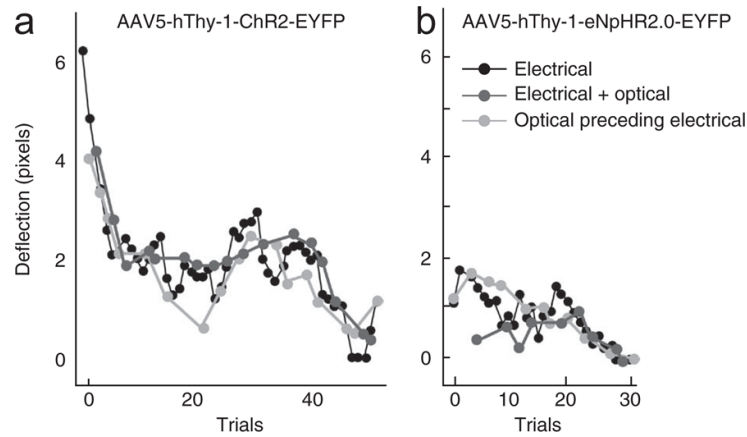
**Figure 2.**

Representative example of electrophysiology results and population summary from the eNpHR2.0-expressing site. **(a)** Raster plots and PSTHs from a light-responsive single unit. The neuron responded with a rapid reduction in firing rate to a train of green laser pulses (20 Hz, 5 ms pulses). The firing rate decreased markedly 2–3 ms after the light pulse (inset). The same neuron showed a complete shutdown of spiking activity during 70–150 Hz pulse trains as well as during continuous illumination with green light (instantaneous power density  $27 \text{ mW mm}^{-2}$ , energy density  $135 \text{ } \mu\text{J mm}^{-2}$  per pulse, average power density  $9.6 \text{ mW mm}^{-2}$  for 1 s complete shutdown caused by 5 ms pulses delivered at 70 Hz; all values refer to the site of electrical recordings; see Online Methods for calculation details). **(b)** Scatter plot of firing rates of all single units and multi-units recorded at the *hThy-1-eNpHR2.0*-expressing area during continuous stimulation versus baseline activity. Empty circles mark non-significant responses to light, filled circles show significant responses. The dashed gray line is the unity-slope line, where baseline firing rate and stimulation firing rate are equal.



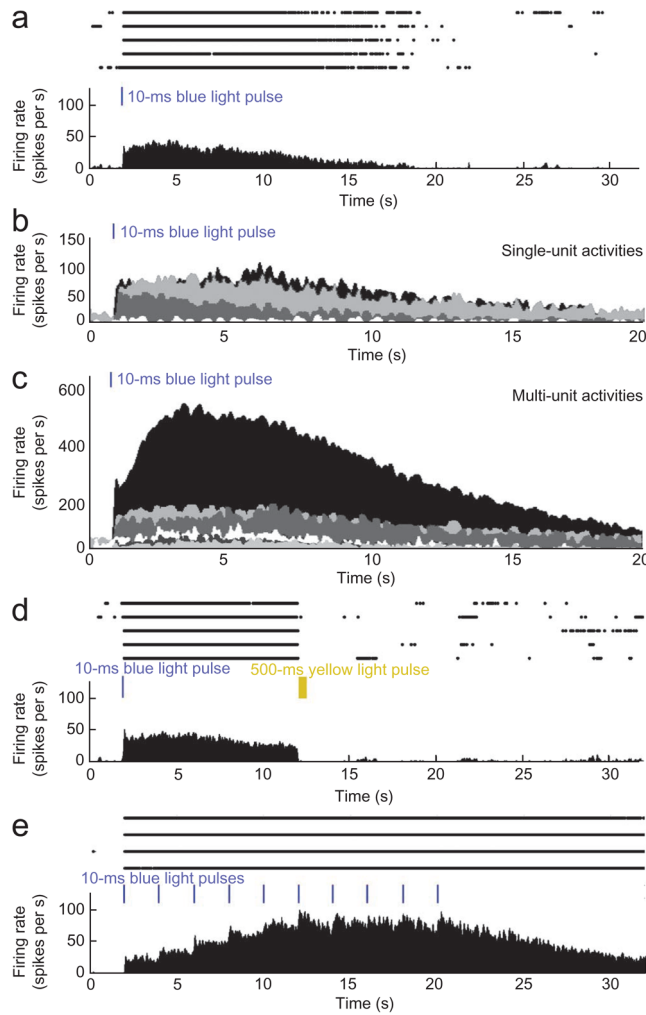
**Figure 3.**

Representative examples of electrophysiology results and population summary from the Chr2-expressing sites. **(a)** Raster plots and PSTHs from a light-responsive single unit at a site injected with AAV5-Syn-ChR2-EYFP stimulated with a power density of  $0.1 \text{ mW mm}^{-2}$ . **(b)** Raster plots and PSTHs from a light-responsive single unit at a site injected with AAV5-hThy-1-ChR2-EYFP stimulated with a power density of  $2.6 \text{ mW mm}^{-2}$ . The pulse-triggered average is plotted with 1-ms resolution illustrating the latency of the suppression or excitation after the light pulse (insets in 20 Hz panel). The reported mean number of spikes per light pulse is a measure of the reliability with which spikes were evoked, corrected for spontaneous spike rate, averaged across the whole stimulation period and all trials. Spikes per pulse represent averages across all trials. **(c, d)** Scatter plots of firing rates of all single units and multi-units recorded at areas injected with *hSyn-ChR2* and *hThy-1-ChR2*, respectively, during continuous stimulation. Firing rates during stimulation are plotted against baseline firing rates (without stimulation). Empty circles mark non-significant responses to light, filled circles significant responses. The dashed gray line is the unity-slope line.



**Figure 4.**

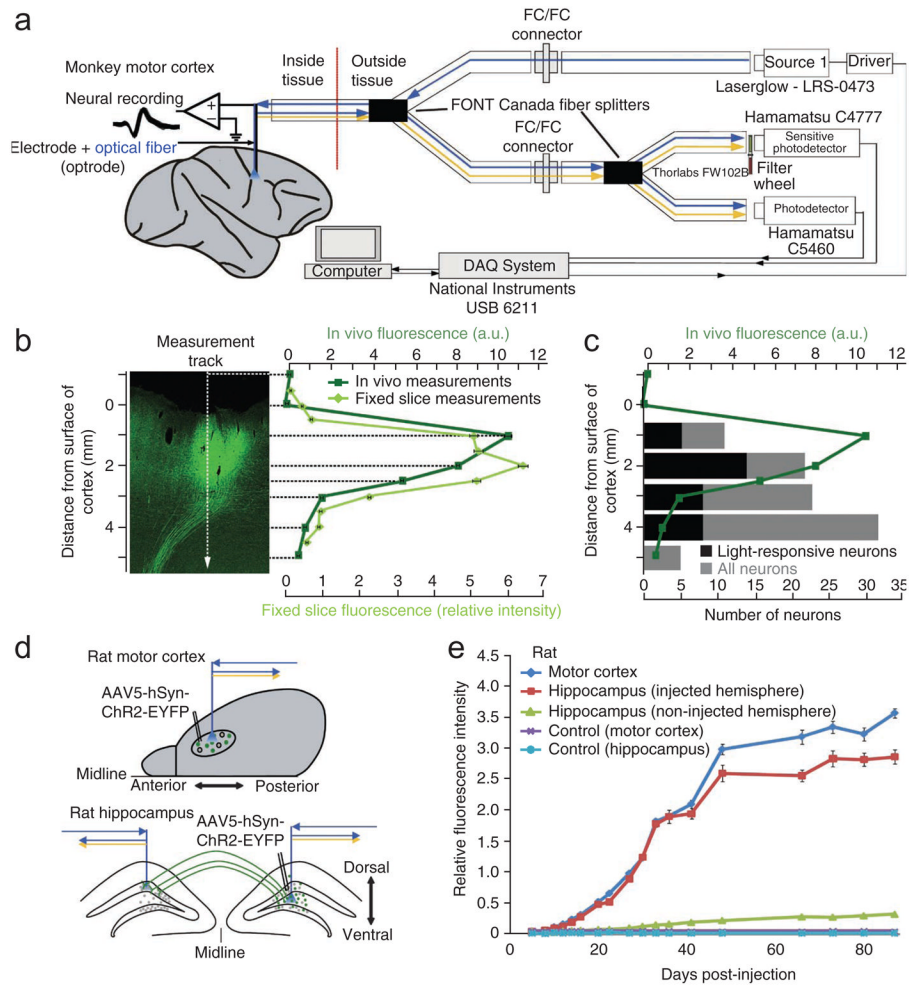
Lack of effect of optical stimulation on passive behavior. **(a)** Electrical ( $50 \mu\text{A}$ ) and optical ( $250 \text{ mW mm}^{-2}$  at the tip of the fiber,  $50 \text{ Hz}$ ,  $3 \text{ ms}$  pulse width) stimulation were both delivered through the same optrode in premotor cortex injected with AAV5-hThy-1-ChR2-EYFP. The amplitude of hand movement caused by electrical stimulations decreased during the course of trials, as is typical with electrical stimulation (black line). Additional simultaneous (dark gray) or preceding optical stimulation (light gray) with blue light neither increased nor decreased the movement, nor did it prolong the efficacy of the electrical stimulation over the course of trials. Optical stimulation alone did not cause any reliable movement (data not shown; no movement observed despite careful observation by I.D. and M.T.K.). **(b)** Electrical ( $35 \mu\text{A}$ ) and optical stimulation ( $250 \text{ mW mm}^{-2}$  at the tip of the fiber, continuous light) delivered to motor cortex injected with AAV5-hThy-1-eNpHR2.0-EYFP. Optical stimulation with green light did not increase or decrease the electrically evoked hand deflections. Note that no graph for ‘optical stimulation only’ is plotted as we did not videotape hand deflection for those trials on days during which we applied the combined optical and electrical stimulation protocol.



**Figure 5.**

Prolonged activation of spiking with a step function opsin (SFO). **(a)** Raster plot (upper) and PSTH (lower) of a single unit from 2 s before until 30 s after a single 10-ms blue light pulse ( $255 \text{ mW mm}^{-2}$ , estimated power density  $20 \text{ mW mm}^{-2}$  at the electrode tip, energy density  $0.2 \text{ mJ mm}^{-2}$ ). Five repeated trials are shown. **(b, c)** PSTHs for all single **(b)** and multi-units **(c)** responding to a single 10-ms pulse of blue light. Each color represents one single or multi-unit. Responses are superposed. **(d)** Neuronal responses of the same neuron as in **a**. Ten seconds after a single 10-ms blue light pulse, we delivered a 500-ms yellow light pulse ( $80 \text{ mW mm}^{-2}$  at the tip of the fiber,  $8.6 \text{ mW mm}^{-2}$  at the tip of the electrode, energy density  $4.3 \text{ mJ mm}^{-2}$ ) that reversed the activating effect of the blue light pulse. Five repeated trials are shown. **(e)** Neuronal responses of the same neuron as in **a**. A train of ten 10-ms blue light pulses was delivered at 2 s intervals. The firing rate increased in a stepwise manner until it reached a plateau after 6 pulses. Four repeated trials are shown.

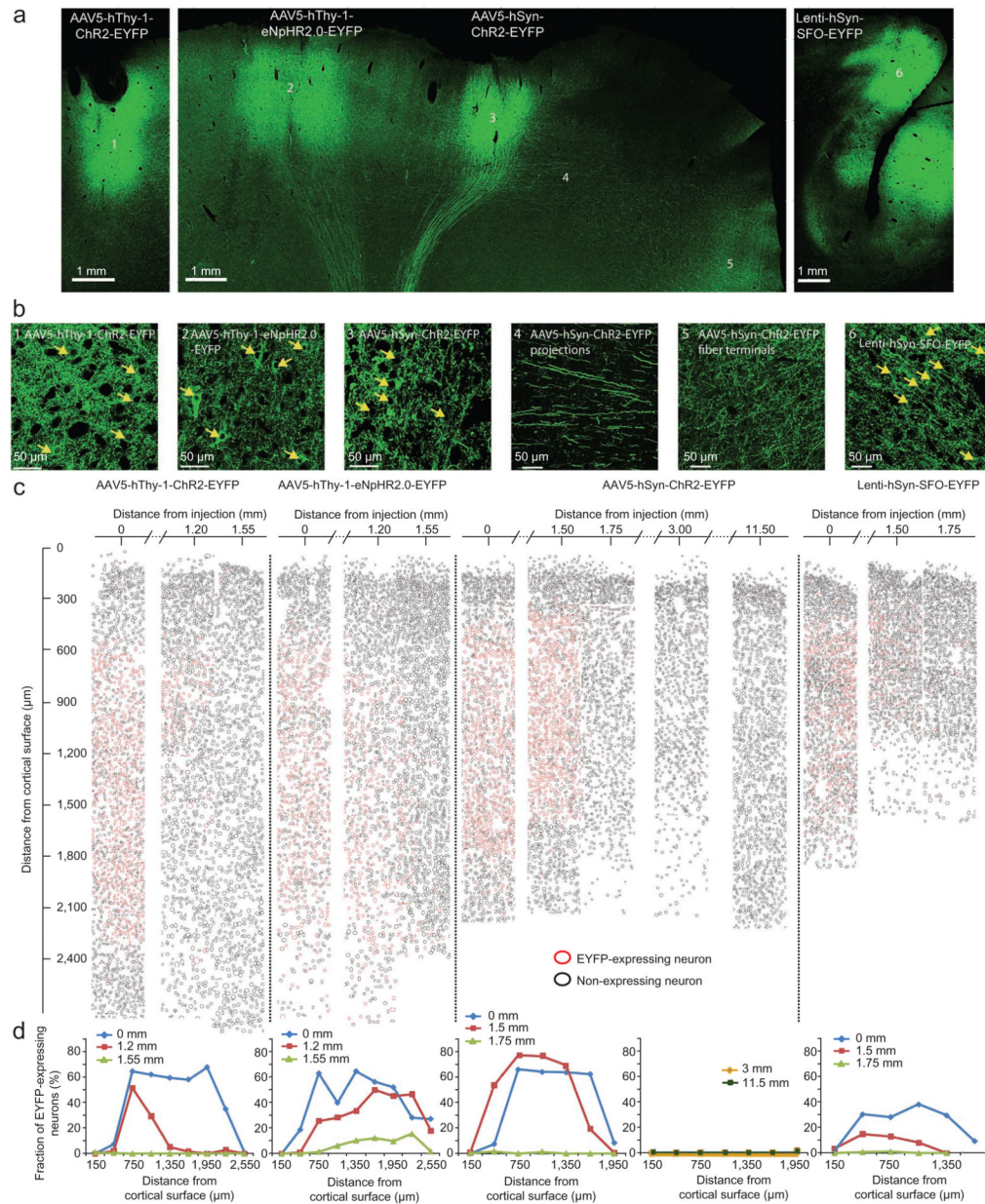




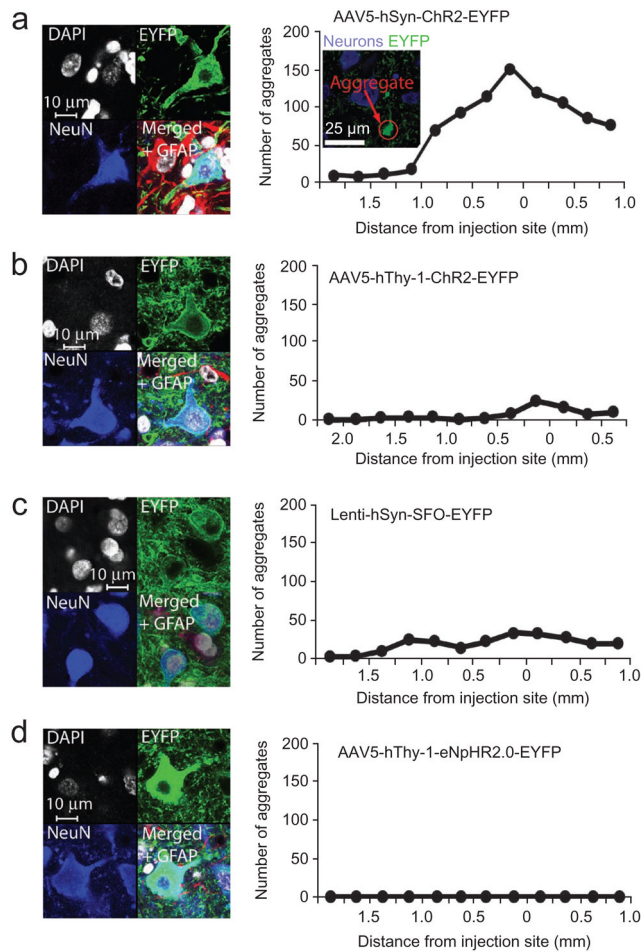
**Figure 6. *In vivo* fluorescence detector and measurements**

(a) Schematic of fluorescence detector. The fluorescence detector system uses fiber splitters to deliver light from multiple laser sources and measures light with multiple detectors. One light source delivers light at the excitation wavelength of the fluorescent molecules in the tissue and one of the detectors has a filter so it measures only the emission wavelength of the fluorescent molecules. The second detector does not have a filter and allows for correction of laser fluctuations and other noise. (b) Image of optogenetically injected and fluorescence detector-probed cortex (left) and associated *in vivo* (dark green) and *in vitro* (measured in the fixed slice; light green) fluorescence measurement (right). For *in vivo* measurements, fluorescence intensities (relative to fluorescence on top of tissue; arbitrary units, a.u.) are plotted against penetration depth in cortex (distance between the surface of cortex and the tip of the fiber; mean  $\pm$  s.d.). For fixed slice measurements the fluorescence values are provided as a ratio of intensity where 1 is the intensity measured from 1 mM of fluorescein dye in phosphate-buffered saline (PBS) (mean  $\pm$  s.d.). An optical fiber connected to the device was moved across the slice using a stereotax. The vertical dashed line indicates the measurement track and the horizontal dashed lines indicate depth of measurements in tissue. (c) Correlation between *in vivo* fluorescence detection and neuronal responses to light at a site injected with AAV5-hSyn-ChR2-EYFP. Relative fluorescence intensities are plotted against penetration depth in cortex. Black, number of light-responsive neurons; gray, total number of recorded neurons at the respective depths. (d) Schematic view of injected brain areas in rats for *in vivo* tracking of fluorescence signal over time and in projecting fibers. (e)

*In vivo* tracking of EYFP expression after injection of AAV5-hSyn-ChR2-EYFP over the course of weeks in rat cortex and hippocampus. Fluorescence values are provided as a ratio of intensity where 1 is the intensity measured from 1 mM of fluorescein dye in PBS (mean  $\pm$  s.d.). Dark blue, injected motor cortex; red, injected hippocampus; green, hippocampus contralateral to injected hippocampus; violet, motor cortex of control (non-injected) rat; light blue, hippocampus of control (non-injected) rat.



**Figure 7.** Histological analysis of cortex. **(a)** Coronal slice through motor cortex injected with AAV5-hThy-1-ChR2-EYFP in monkey D (left), coronal slice through motor cortex injected with AAV5-hThy-1-eNpHR2.0-EYFP and AAV5-hSyn-ChR2-EYFP, respectively, in monkey D (middle), and sagittal slice through area PE injected with Lenti-hSyn-SFO-EYFP in monkey B (right). **(b)** Magnified views of the injected areas (indicated by numbers 1, 2, 3 and 6) and areas that receive projecting fibers (4 and 5). Arrows point out single EYFP-opsin expressing neurons. **(c)** Evaluation of efficiency of viruses. Red circles represent EYFP-expressing neurons, black circles depict non-EYFP-expressing neurons. Efficiency was evaluated across all cortical layers and at different distances from the center of injections. **(d)** Efficiency as a function of cortical layer. Different curves represent distances from center of injections.

**Figure 8.**

Evaluation of cell health. **(a)** Cell nucleus (DAPI, gray/white), neuronal (NeuN, blue) and astroglia (GFAP, red) cell staining at a site injected with AAV5-hSyn-ChR2-EYFP (left). Distribution of aggregations in a site injected with AAV5-hSyn-ChR2-EYFP as a function of the distance from the center of injections (right). Inset, example picture of aggregates in the center of injection of a site injected with AAV5-hSyn-ChR2-EYFP. **(b–d)** DAPI, NeuN and GFAP staining and aggregate distribution at sites injected with AAV5-hThy-1-ChR2-EYFP **(b)**, Lenti-hSyn-SFO-EYFP **(c)** and AAV5-hThy-1-eNpHR2.0-EYFP **(d)**.